Anisotropy Pinning of Domain Walls in a Soft Amorphous Magnetic Material

Rudolf Schäfer, Wing K. Ho, Jiro Yamasaki, Alex Hubert, and Floyd B. Humphrey

Abstract—**Annealing short very low magnetostriction amorphous ribbons in the demagnetized state results in a Perminvar-like reentrant hysteresis loop due to domain wall stabilization by the induced anisotropy. After a hard saturation, the loop changes to that of an unprocessed ribbon. In this investigation, ribbons are annealed in the demagnetized state with one wall along the ribbon middle. This wall becomes pinned during the heat treatment. Reentrant reversal occurs when reverse domains are nucleated at the ribbon edge with a threshold field larger than the demagnetizing field, this wall does not annihilate when it meets the pinned wall but leaves a line of reverse domains stabilized by ripple in the anisortopy. These domains enable a regular smooth reversal for the demagnetization process until the ribbon returns to the pinned configuration. The regular loop appears when the ribbon has been completely saturated by a large field. Mobile walls are nucleated on both sides of the pinned wall so that the ribbon does not return to the pinned configuration. Reversal now follows the usual demagnetization curve over the entire cycle. Kerr magnetooptical domain and domain wall observations are used in this investigation. All of the possible wall structures predicted by the model of asymmetric flux closed Bloch walls were identified.**

I. Introduction

It is well known that mechanical stresses in amorphous alloys can significantly affect their soft magnetic properties because of magnetostrictive interactions. A generally held procedure for ribbons made by melt spinning is to include a stress relief anneal in a field high enough to saturate the ribbon. This procedure is used even if the material is of a nonmagnetostrictive composition. Fujimori *et al.* [1] compared amorphous samples treated in this way with samples that were annealed in the absence of a magnetic field. In the latter case, they found enhanced losses and a characteristic Perminvar-type hysteresis loop, which they attributed to an induced anisotropy due to pair ordering in the metallic glass [2]. This effect was assumed to stabilize the domain wall pattern of the demagnetized state. The authors also record the fact that the nature of the hysteresis loop can be changed by applying a strong field (Fig. 3 of [1]) without offering an explanation of this observation. The results of similar experiments with longer annealing times in short segments of very low magnetostriction ribbon were published and the stabilized pinned domain walls were confirmed by domain observation [3]. An attempt to relate the observed coercivity of the Perminvar loop as a function of the ribbon composition with the calculated pinning field of domain walls due to the induced anisotropy resulted in a qualitative agreement. However, the stabilized domain pattern broke up at much lower fields than calculated. An analogous behavior was obtained in amorphous sputtered thin films [4] when they were annealed in the absence of a magnetic field.

In this paper, narrow very low magnetostriction amorphous ribbons that have been annealed in their demagnetized state are investigated. In these samples the heat treatment stabilizes a domain pattern that is usually simple with only one domain wall along the middle of the ribbon. The ribbons display a Perminvar-like reentrant hysteresis loop. This loop can be transformed into a regular hysteresis loop after the application of a 100 Oe field along the ribbon axis. We try to clarify the origin of this change of hysteresis loop by domain and wall observations using Kerr magnetooptical effect. Kerr magnetooptic images used for this investigation rely on the technique of digital background subtraction and contrast enhancement [5]. In this study we will show that the properties of these walls and the transitions within them play an essential role in the explanation of the observed unusual hysteresis behavior in "bulk" amorphous strips.

In the course of this study we have identified all the possible wall configurations and transitions of walls in metallic glass observable in the Kerr microscope that are predicted by the stray field-free model of Bloch walls in soft magnetic materials [6]. This model assumes that the domain walls avoid strong stray fields at the sample surface by forming a vortex on one side of the wall or the other to provide flux continuity for the magnetization in the center of the Bloch wall. Near the surface, the vortex resembles a Néel wall. Vertical Bloch lines, where the chirality of the Bloch wall changes, have been identified as well as vortex switch structures where the vortex flips to the other side of the wall. Up to now wall observations by magneto-optical means have been performed in film structures mainly for thin film heads which are not thick enough to show all of these effects [7]–[8].

Manuscript received June 22, 1990; revised January 21, 1991.

R. Schäfer and A. Hubert are with the Institute for Materials Science of the University of Erlanger-Nurnberg, D852 Erlangen, Federal Republic of Germany.

W. Ho is with Sensormatic Electronics, Deerfield Beach, FL 33442.

J. Yamasaki is with the Kyushu Institute of Technology, Tobata, Kitakyushu 804, Japan.

F. B. Humphrey is with the ECS Department, Boston University, Boston, MA 02215.

IEEE Log Number 9144745.

II. Experimental

Very low mangetostriction ribbons with a cross section of 40 × 1000 μm and a nominal composition of $(Co_{0.94}Fe_{0.06})_{79}Si_6B_{15}$ were cut to a length of 5 cm. They were first stress relief annealed at 300°C for 30 min in a saturating field of 100 Oe along their length. Then they were demagnetized at a frequency of 10 Hz. Only ribbons with a hysteresis loop that showed straight parallel sides leading smartly to saturation with an H_c of about 10 mOe were used. The demagnetizing field was about 0.5 Oe. The demagnetized ribbons were then annealed at 300°C for 30 min in a field-free environment to produce wall pinning. Both anneals were done in dry N_2 to minimize surface oxidation. The ribbons were finally given an antireflection coating of ZnS to improve the Kerr contrast. Exposure of the ribbons to any field higher than 3 Oe before domain observations was avoided so that any irreversible change on the wall pinning by the external field was minimized.

Domain and wall observations were made on the air side of the ribbons using the magnetooptical Kerr effect with video image enhancement described in more detail previously [5]. The samples were mounted in a solenoid modified with an opening for observation. It generated fields up to 100 Oe, uniform within 3% on its axis over a length of 10 cm. Wall observations were made using a 100× oil immersion objective lens with a numerical aperture of 1.25. In all the pictures, the ribbon axis and the easy axis of anisotropy are oriented horizontally but perpendicular to the plane of incidence of the microscope. The transverse Kerr effect is sensitive to the magnetization components along the ribbon axis in this arrangement and was therefore used for the observation of the basic domains, while the longitudinal Kerr effect was used for the wall observations. Background for the image enhancement was usually obtained by saturating the sample. Occasionally, it was desirable to observe the domains before any field was applied. In this case, the domain or wall pattern was taken as "background" to be subtracted from the afterwards saturated sample resulting in an image with reverse contrast.

The hysteresis loop is recorded simultaneously with a pickup coil. This allows us to correlate the observed domain patterns with the current hysteresis status. If the pinned hysteresis is changed in the course of domain observation due to large fields in connection with the difference image technique, the application of high field pulses occasionally restores the constricted loop, thus allowing repeated experiments on the same sample.

III. Results and Discussion

A. Hysteresis Loops

The hysteresis loop of a very low magnetostriction amorphous ribbon after the field-free anneal is shown in Fig. 1(a). The characteristic pinned state followed by reentrant reversal above a threshold is the same as seen by others [1], [3], [4]. The loop seen in Fig. 1(b) is after the application of a 100 Oe field in the longitudinal direction. The Perminvar-like loop changes to a regular loop with the shape that would be expected for a short length of ribbon. The low coercive force and the continuous character of the loop are the same as just after the stress relief anneal.

B. Low-Resolution Observation of Magnetic Domains

The domain patterns for a typical field-free annealed ribbon near the center of the ribbon as observed utilizing the transverse Kerr effect are shown in Fig. 2. Patterns were observed corresponding to various places on the hysteresis loop. The demagnetized ribbon is shown in Fig. 2(a) and Fig. 2(e). Presumably, this was the domain pattern during the field-free anneal. A particularly simple domain pattern was chosen for this illustration. However, most samples are nearly this simple, depending, of course, on the care in removing the sample from the loop tracer and the success in avoiding the earth's field. During the anneal, a pinning site has been established and it is indicated on the domain pictures. When a field exceeding the threshold is applied, a wall pops into view from the edge as seen in Fig. 2(b) and Fig. 2(f). This is the reentrant portion of the loop. As the field is increased, the walls move smoothly toward saturation, leaving reverse domains along the pinning site as seen in Fig. 2(c) and 2(g). When the field is reduced, the walls from the reverse domains move smoothly back (Fig. 2(d) and 2(h)). Once the field reaches zero, the walls will reach the sample edge and only pinned walls exist in the sample. The process is ready to start again.

Characteristic domain patterns of a ribbon after being saturated in a 100 Oe field are shown in Fig. 3. Coming back from saturation, reverse domains are nucleated on both sides of the pinning site (Fig. 3(a)). As the field is further reduced, the walls move smoothly away from the pinning site (Fig. 3(b), (c)) to remagnetize both halves of the sample simultaneously. At some places along the pinning site, little residual domains are left similar to those in Fig. 2(g), except that this time the residual domains are on both sides of the pinning site. The pinning site is now in a similar state as at the beginning and ready for reversal in the other direction following the same mechanism (Fig. 3(d), (e)).

To fully understand the mechanism, a number of questions should be answered.

- How does the nucleation occur at the sample edge?
- Why do the free and pinned walls not annihilate totally near saturation in the Perminvar loop, but leave residual domains along the pinning site, which act as nuclei for reversal? The residual domains localized on one side of the pinning site are important for the maintenance of the reentrant loop.
- What is the role of the pinning site after saturation of the pinned wall by a high field? What can be said about the mode of nucleation at the pinning site?

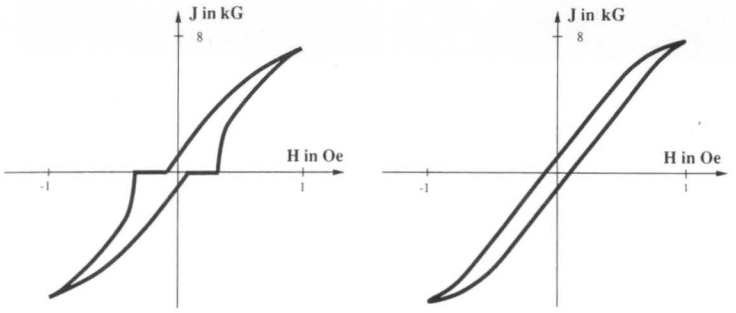

(a) (b)

Fig. 1. Hysteresis loops of a magnetostriction free metallic glass measured at 50 Hz (a) after annealing in the demagnetized state and (b) after saturation in a high field.

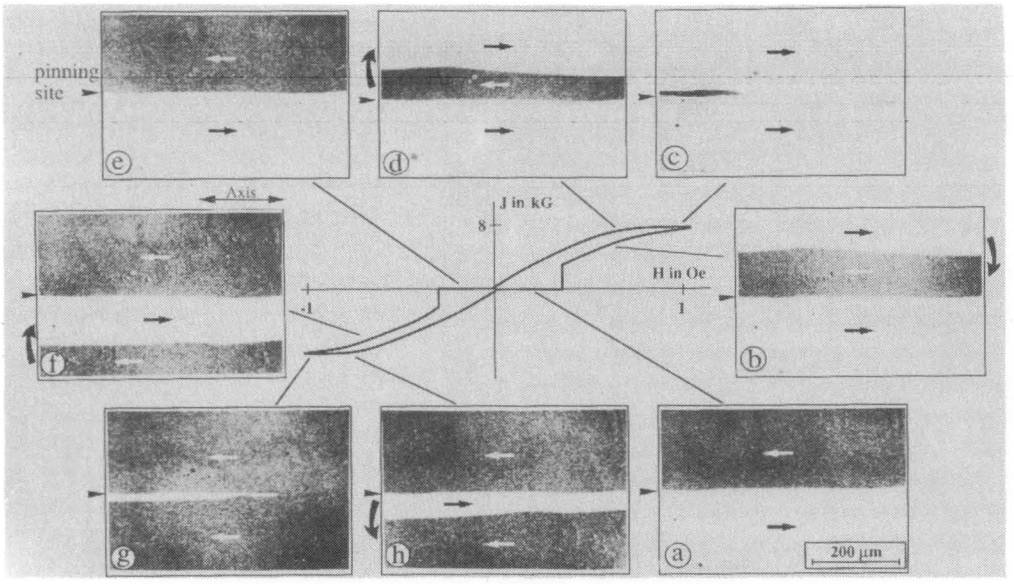

Fig. 2. Kerr magnetooptic micrographs of the domain configuration in a ribbon annealed to exhibit a Perminvar loop for various applied fields corresponding to positions on the loop as indicated: (a) demagnetized and pinned, (b) magnetized to the right after reentrant reversal, (c) saturated to the right, (d) partially saturated, (e) demagnetized and pinned, (f) magnetized to the left after reentrant reversal, (g) saturated to the left, (h) partially saturated. The pinning site is marked with arrow heads, the magnetization direction by straight arrows, and the wall motion direction by curved arrows.

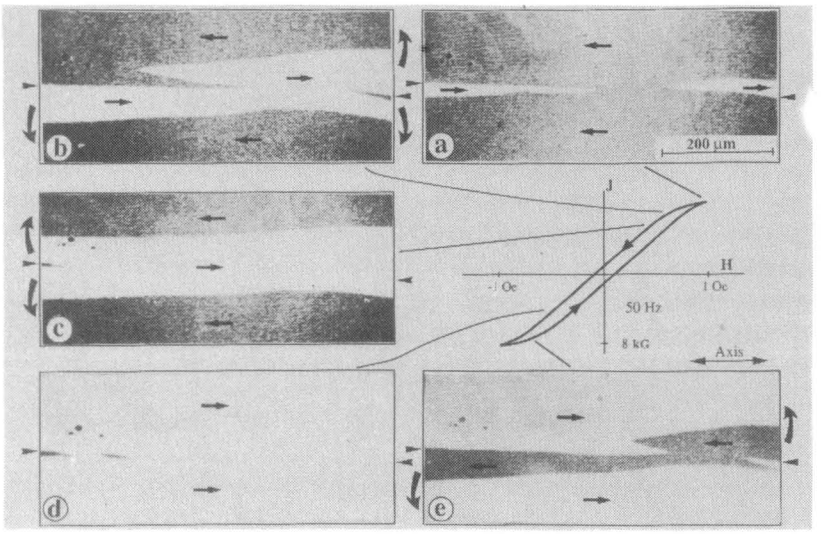

Fig. 3. Kerr magnetooptic micrograph of the domain configuration in a ribbon after the application of a high axial field: (a) reverse domain at soft saturation, (b) partial saturation, (c) residual domain at partial saturation, (d) residual domains at soft saturation, (e) reverse by residual domains. The pinning site is marked with arrow heads, the magnetization direction by straight arrows, and the wall motion direction by curved arrows.

In order to answer the questions we now turn to high-resolution wall observations.

C. High Resolution Analysis of Domain Walls

By switching to the longitudinal Kerr effect with the same sample orientation as above, and by using oil immersion, the walls can be made visible in the microscope. Various kinds of walls will be shown in Figs. 5–7. They appear as black or white lines between the antiparallel domains, which appear grey under these conditions of the microsope. The black and white contrast signify that the walls on the surface are magnetized in a direction perpendicular to the wall. This is in agreement with the model of the asymmetric Bloch wall [6] with its characteristic vortices near the surfaces. Looking ahead to Fig. 5, one gets an idea of the internal structure of these walls. There we see that what is indicated as the pinned wall is much wider than the free wall. In Fig. 4, the magnetooptic signal is plotted as a function of distance perpendicular to both types of walls. The width of the walls is calculated by integrating across the wall the magnetooptic signal relative to the gray magnetooptic signal level when the magnetization is pointing orthogonal to the direction of observation, normalized by the domain intensity [9]. The domain intensity is defined as the difference of magnetooptic signal when magnetization is pointing parallel and orthogonal to the direction of observation. The wall width is found to be 0.9 μm for the free wall and 1.7 μm for the pinned wall.

The width of the pinned wall, about twice that of the free wall, is explained by the reduction of anisotropy energy of the pinned wall because of the rotation of local anisotropy axis to fit the wall shape. The exchange energy reduces accordingly by an increase in the wall width to balance the reduction of anisotropy energy. The situation in metallic glasses differs from regular crystalline materials where the induced anisotropy is usually superimposed over a stronger crystalline anisotropy. Here the anisotropy axis can rotate completely inside the wall, which leads to the change in the wall width due to annealing. The anomalous behavior of domain walls under conditions of predominant induced anisotropy have been studied previously in cobalt-doped ferrites by Paulus *et al.* [10] and in metallic glasses by Aroca *et al.* [11].

All possible wall structures in the free and pinned wall are seen in Fig. 5(a) using high resolution Kerr microscopy. The various structures are labeled on the schematic for the pinned wall seen in Fig. 5(b). Presumably, they were present in the wall already at the time of anneal. The details of the observed surface pattern of the walls can be understood with the model of the asymmetric Bloch wall. As mentioned, the principle of this model is that of flux closure. The closure causes a vortex on one side of the wall and a Néel-like cap on each surface. Only this cap is observed in the longitudinal Kerr effect with the plane of incidence perpendicular to the wall. The four equivalent orientations of the wall O1–O4 are shown schematically

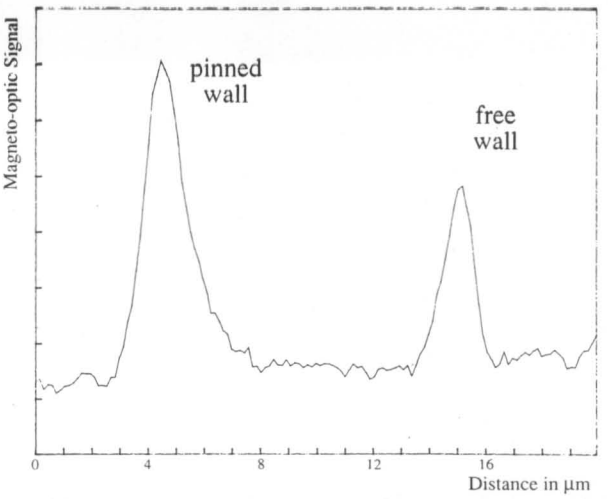

Fig. 4. Optical profile of a free and a pinned wall. The wall width is 0.9 and 1.7 μm, respectively.

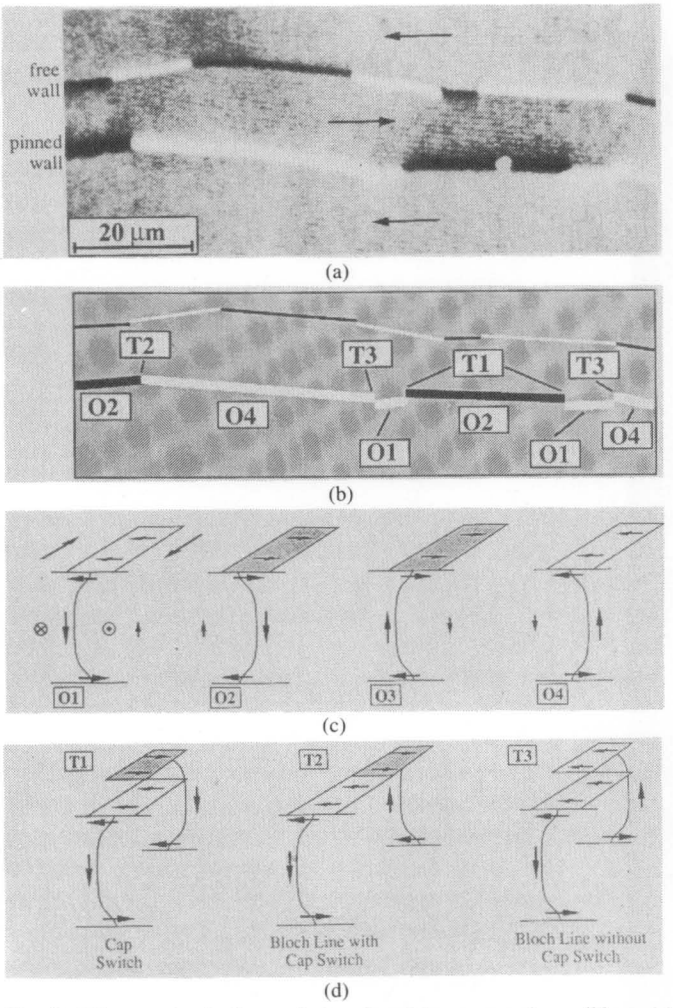

Fig. 5. Micrograph of a free and pinned wall in an amorphous ribbon: (a) high resolution Kerr magnetooptic, (b) identification of the different wall segments and transitions. Schematic of the (c) possible wall structures and (d) basic wall transitions.

in Fig. 5(c) as cross sections over the sample thickness. For each wall cross section the domain magnetization is pointing into the paper on the left and out on the right. The chirality of the wall is indicated by the direction of

the center spin of the wall, shown by the large arrow pointing downward for O1 and O2 in Fig. 5(c), with the other two opposite. This flux can close on either the right or the left side of the wall as indicated by the small arrows. The direction of this vortex determines the direction of the magnetization in the surface wall cap. The cap is centered over the vortex and, therefore, offset from the center of the wall towards the vortex core.

Since all four possible orientations of the asymmetric Bloch wall are energetically equivalent, they are equally likely to occur. If it is assumed that these structures are also equally likely to exist in the same wall, then there are three basic types of possible transitions from one wall segment to another. They are shown as T1 to T3 in Fig. 5(d). The first transition T1 is indicated along a down chirality wall, where the vortex changes from the right to the left side. This would be a transition from wall structure O1 to O2. This vortex switch is observed as a cap switch, i.e., a change in all contrast on the surface, accompanied by a jog along the wall. Of couse, a transition from wall structure O3 to O4 also corresponds to transition T1. Transition T2 assumes a change in chirality of the wall, i.e., a vertical Bloch line (VBL) at the transition with the vortex remaining on the same side of the wall. Such a transition results by combining O1 with O3 or O2 with O4. For this case a cap switch caused by the change in chirality of the Bloch wall but without a jog is observed. Finally, transition T3 also assumes a VBL but with the vortices on opposite sides of the wall for each wall segment. Transitions between structure O1 and O4 would give a jog in a bright stripe and between O2 and O4 would be a jog in a dark stripe.

A typical kink at the surface can be seen in the walls with wall transitions, which we have identified as VBL's in the interior. This strong deformation of the straight wall near Bloch lines is a characteristic feature of thick films and bulk material as was first explained by Shtrikman and Treves [12]. The kinks at the surface allow a distribution of the flux of one wall segment to the neighboring segments of opposite chirality as illustrated in Fig. 6. For simplicity the surface vortices of Fig. 5 have been omitted in this diagram. A part of the wall flux is transported parallel to the surface along the wall, rather than to the bottom surface as in the simple model of the asymmetric Bloch wall. So the division into a multipolar wall together with the kinking at the surface results in a reduction of the total energy of the wall for thick films and for bulk samples.

To confirm that the kinked transitions T2 and T3 contain Bloch lines, an experiment similar to one by Hartmann and Mende [13] was performed. External fields of about 100 Oe were applied perpendicular to the ribbon surface. The effective internal field resulting from this external field does not move the wall if oriented carefully. Wall segments magnetized along the field direction will expand, at the expense of segments with opposite magnetization, by the movement of the VBL's. Results are shown in Fig. 7.

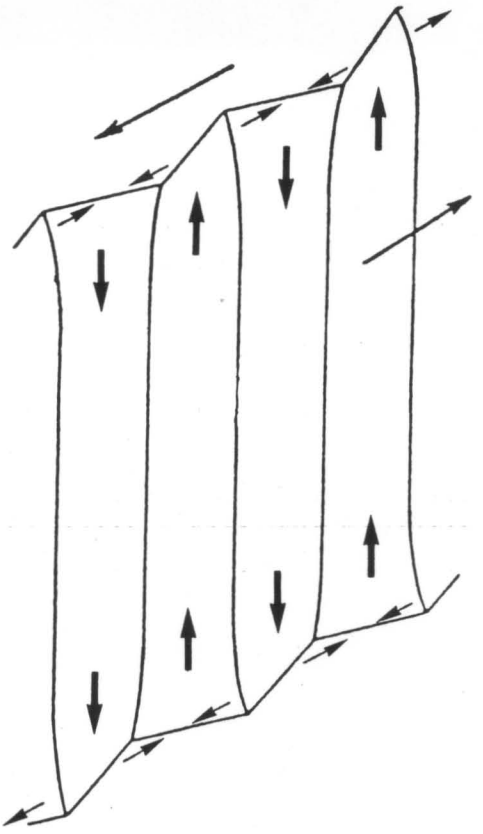

Fig. 6. The model of Shtrikman and Treves [12] for the three-dimensional flux distribution in the segmented Bloch wall. The domain wall is shown with the same perspective as in Fig. 5(c) and Fig. 5(d). Vertical arrows indicate the chirality of wall. Other arrows indicate bulk magnetization in the domain.

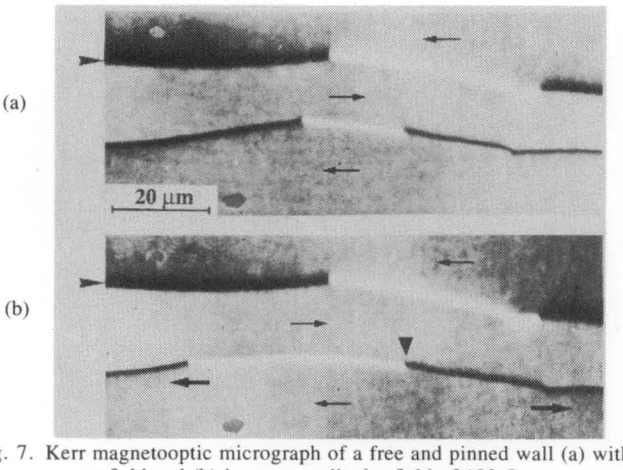

Fig. 7. Kerr magnetooptic micrograph of a free and pinned wall (a) without field and (b) in a perpendicular field of 100 Oe.

In both pictures a pinned (upper) and a free wall (lower) can be seen. The free wall has a VBL transition type **T2** to the left and a VBL transition type **T3** to the right, with a cap switch transition type **T1** between them. After the application of a 100 Oe field perpendicular to the ribbon surface, the picture of Fig. 7(a) changed to that of Fig. 7(b). It can be seen that both kinked VBL transitions in the free wall have moved in opposite directions. When the field is reversed, the two VBL transitions move back. The

cap switch **T1** in the middle, which does not carry a Bloch line, is stationary. The structures in the pinned wall are also stationary due to the stabilization that is provided by local induced anisotropy. This observation constitutes further confirmation that the assignment of structure in Fig. 5 is correct.

D. Micromagnetic Structures of the Pinning Site

In order to understand the reactions of walls in the two hysteresis states, we next have to look at the possible configurations of the pinning site. This area, where the annealed-in anisotropy makes a twist, plays a central role in both modes. In the Perminvar mode the pinning site must hold a pinned wall securely to force nucleation at the edge. After the application of a large field it is a nucleation site that provides free walls for the continuous reversal of the sample. All possible structures of the pinning site must be related somehow to the twisted anisotropy, which follows the profile of the asymmetric Bloch wall that sat at this location during annealing. We will restrict our models to the surface structures of the pinning site, because this is what we see in the microscope. Corresponding considerations apply for the unobservable interior.

Fig. 8 shows three different residual domains nucleated at different times at the same pinning site in highest resolution. The weak light-and-dark contrast of Fig. 8(a) appears close to saturation, with no residual domains visible. This zero degree wall-like structure, sitting in a domain, is called a "quasi-wall." All kinks and cap switches of the original wali are also recognizable in the quasi-wall. The residual domains seen in Fig. 8(b) to Fig. 8(d) are of the kind seen in Figs. 2 or 3. In Fig. 8(b) and 8(c) a part of the pinning site is occupied by regular, stable pinned walls whose magnetization follows the direction of induced anisotropy. It is observed that the contrast of a stable pinned wall depends on the domain magnetization on both sides of the wall as shown in Fig. 8(b) and 8(c). Due to the unaxial nature of induced anisotropy, the twisted anisotropy can accommodate walls with opposite magnetization at every point equally well. In Fig. 8(d) an unstable wall was formed in the pinning site. It is the result of a wall that enters the pinning site with a chirality opposite to the chirality of the site. This wall with its characteristic black-and-white contrast usually switches to the stable configuration in the course of the magnetization process.

Optical profiles of different pinned wall images are shown in Fig. 9. An asymmetric profile is recognizable. The line scans reflect only the transverse magnetization component of the walls. They agree qualitatively with what one would expect based on the asymmetric annealed-in anisotropy profile in the surface. A schematic of the anisotropy profile is shown in Fig. 10. The angle of magnetization is plotted as a function of distance across the wall in Fig. 10(a). The value $\vartheta = 0$ stands for magnetization to the right, and the value $\vartheta = \pi$, stands for magnetization to the left. The hypothetical easy directions

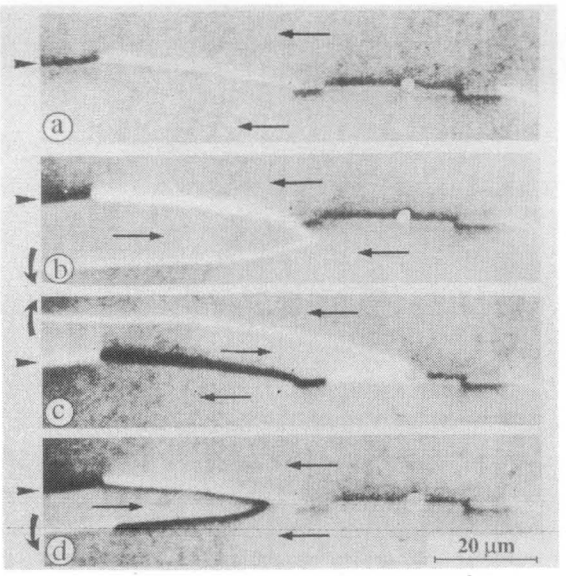

Fig. 8. Different residual domains at the same pinning site. (a) Pinning state as a quasi-wall before domains are nucleated. (b) to (d) Various residual domains spreading along the pinning site.

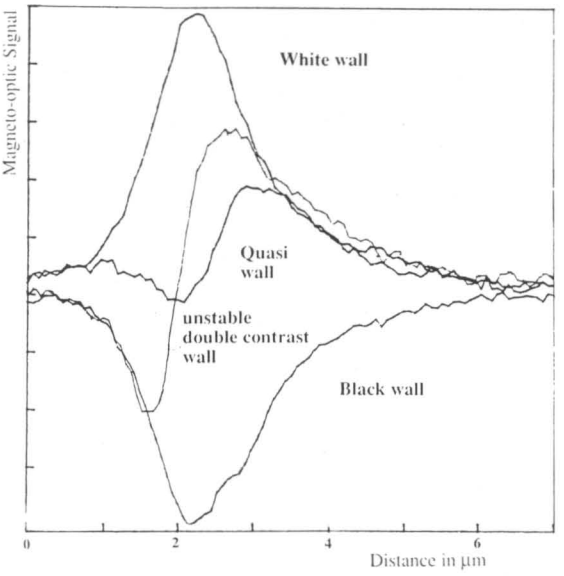

Fig. 9. Optical profiles measured perpendicular to the wall across the four different structures of a pinning site.

at the pinning site are indicated in grey in each case. In Fig. 10(b) the same contours are shown pictorially including the wall contrast as it would appear in the longitudinal Kerr effect. Both the black and white wall simply follow the annealed-in anisotropy. Thus the contrast is determined by the anisotropy and the sign of the domain magnetization. The unstable wall differs from the corresponding stable wall by its opposite net rotation sense. The magnetization deviates at two places from the easy direction. Therefore, it transforms easily into one of the stable states. The model also explains the weakly visible asymmetric dark-and-light contrast of the quasi-wall. In the middle of this double contrast the magnetization is perpendicular to the local easy axis. Thus the quasi-wall is a suitable starting point for nucleation.

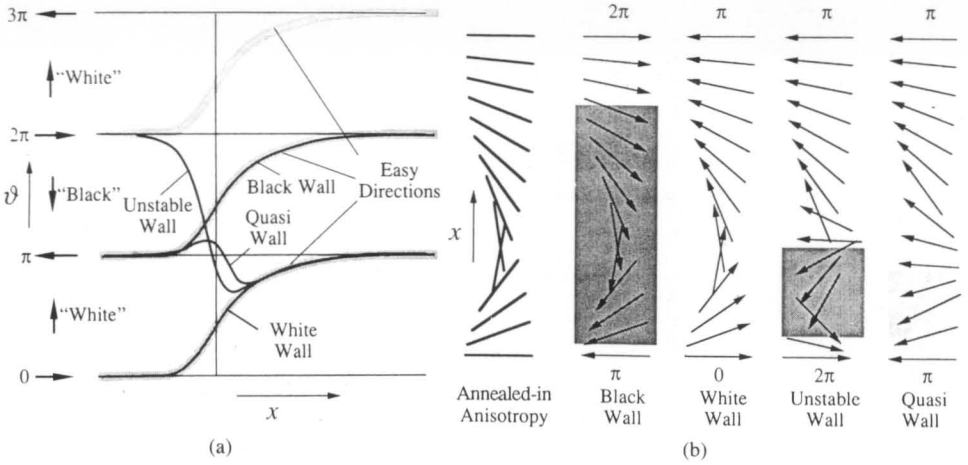

Fig. 10. Surface wall contours of the different observed wall types at the pinning site (a) plotted as angle for different position across the wall, (b) presented as arrow plot. The schematics are based on the asymmetric Bloch wall model.

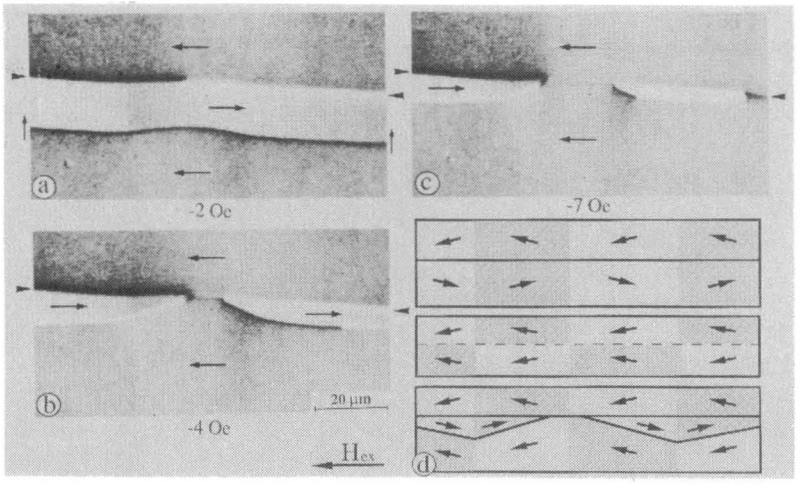

Fig. 11. Kerr magnetooptic micrograph of a free wall moving towards the pinned wall (a) before the two walls meet, (b) just after walls meet, and (c) after residual domains are well formed. (d) Schematic of the ripple-like modulation of the annealed-in anisotropy responsible for the residual domains.

E. Mechanism of the Pinned Loop

1. Nature of the Residual Domains: Fig. 11 shows the formation of residual domains in high resolution. In Fig. 11(a), a structureless free wall approaches the pinned wall from the bottom. It was nucleated somewhere at the sample edge and jumped in after reaching the threshold for remagnetization. As the free wall meets the pinned wall, the two walls annihilate in the center, leaving behind a short section of quasi-wall (Fig. 11(b)). Annihilation is obviously impeded on both sides. The two residual domains that were created are quite stable as can be seen in Fig. 11(c), where a field of -7 Oe is applied. The residual domains act as nuclei for remagnetization.

It seems that the residual domains are stabilized by a ripple-like modulation of the anisotropy in the domains. It was annealed into the ribbon during the field-free anneal. The ripple is visible in the photographs as a long-wavelength dark-and-light shading extending perpendicularly to the sample axis. Fig. 11(d) is a schematic illustrating how this stabilization might work. At the top is the pinned wall with the long-range ripple corresponding to the structure in the photos. The ripple has the same shade on either side of the wall. Since the longitudinal Kerr effect is sensitive to the magnetization component perpendicular to the wall under the circumstances of the experiment, this means that the annealed-in easy directions to the left and the right of the wall are inclined to each other. Thus the angle of magnetization with respect to the pinned wall is the same on both sides and the wall is stray field-free. If now a free wall approaches the pinned wall, and if both walls would annihilate over their whole length, a charged state would be created at the quasi-wall as sketched in the middle of Fig. 11(d). Those charges can be avoided by leaving residual domains at the pinning site as illustrated in the lower diagram of Fig. 11(d). They allow a stray field-free magnetization to follow everywhere the local easy axis. Ripple-like excursions in the

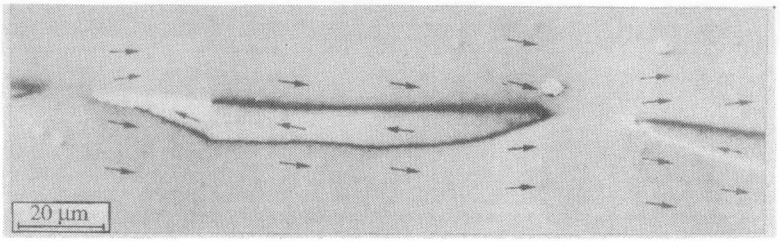

Fig. 12. Quantitative analysis of the residual domain structure. The upper wall of the domain is a pinned wall and the lower wall is free.

domain magnetization can often, but not always, be observed in association with transitions in the pinned wall. One hypothesis that needs further study is that the observed deviations in the domain magnetization have been generated as a consequence of wall transitions during the annealing.

With quantitative Kerr microscopy [14] we can confirm the model for the residual domains. With this method we are able to derive, quantitatively, the magnetization direction at every point of the sample surface by comparing the actual domain or wall intensity with intensities of well-defined saturated states. The result of such an analysis is shown in Fig. 12. Normally we use a color wheel to define the measured magnetization directions. Since a color presentation is not possible in this publication, the magnetization direction of the most important points in Fig. 12 are indicated by arrows. The picture shows residual domains that have been formed with a free wall (lower) moving from the bottom side towards the pinned wall (upper). The strong deviations of the magnetization directions from the sample axis, which were indicated by the dark-and-light shading in Fig. 11, are clearly observed. At the ends of the central residual domain, two ripple zones are visible that are responsible for the existence of this domain as depicted in Fig. 11(d). The two ripple zones of the central domain are connected by an undisturbed straight region of anisotropy on both sides of the pinning site. Based on the arguments explained in Fig. 6, we see that the two Bloch walls here have the same internal rotation sense, leading to a repulsive interaction of the walls in that area. From this observation we can conclude that Bloch wall attraction and repulsion can modulate the basic ripple mechanism of the residual domains.

The reaction of a free wall with the pinned wall is not everywhere as reproducible and clear as would be expected from the ripple effect only. An example is demonstrated in Fig. 13. Here a structureless free wall meets the pinned wall from the bottom (Fig. 13(a) and 13(b)). The pinned wall has a VBL at both ends and a cap switch in the middle. At this location we observed two possibilities that occurred with the same frequency. In Fig. 13(c) the two walls have annihilated, leaving behind a "quasi-wall" over the whole field of vision. It seems that the annihilation starts at the left VBL of the pinned wall to spread over a larger area of the pinning site. In the other case a similar looking free wall is suddenly repelled and a pair of Bloch lines is generated (Fig. 13(d)). This leads

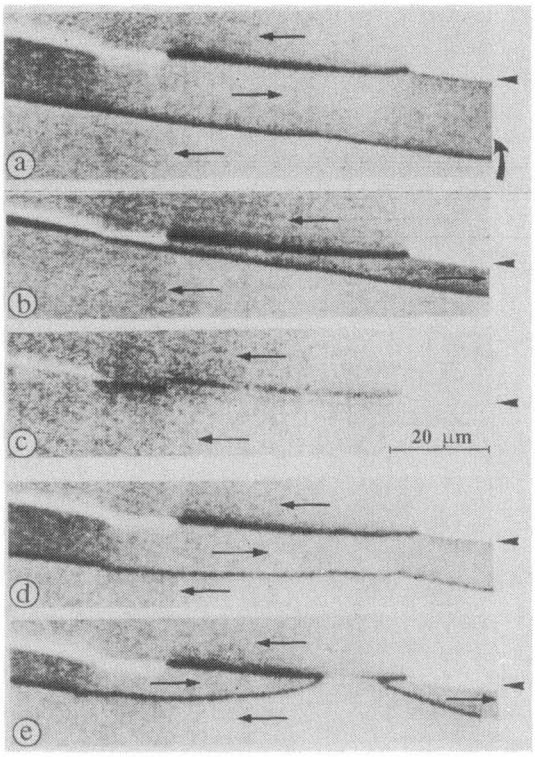

Fig. 13. Kerr magnetooptic micrograph of (a) a free wall moving towards a pinned wall, (b) as the walls meet, (c) resulting in a quasi-wall, or (d) another wall at the same site (e) results in the formation of residual domains.

to a strong kinking of the free wall similar as in the pinned wall. Now all segments with equal internal chirality are facing each other and repel each other, and they need higher fields for an approach. Thus residual domains are found in this case (Fig. 13(e)).

2. *Nucleation at the Sample Edge:* In connection with the mechanism of the Perminvar loop we finally have to answer the question of how the domains are nucleated at the sample edge. They are responsible for the reentrant reversal. As possible nuclei we discovered at some places little domains extending along the sample edge with a width of 20–50 μm and several 100 μm long. They are only visible at high magnification and cannot be detected by the domain observations at low resolution (Fig. 2) because of the curvature of the sample edge. A part of such an edge domain is shown in Fig. 14. It appears that nucleation from annealed-in edge domains is relatively easy (Fig. 14(b)). The free wall thus created does not spread immediately, however. Rather, it seems to be pinned by

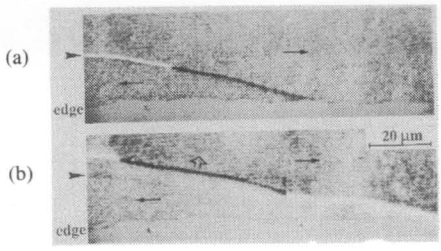

Fig. 14. Kerr magnetooptic micrograph of (a) a domain at the sample edge, and (b) which has left its pinning site.

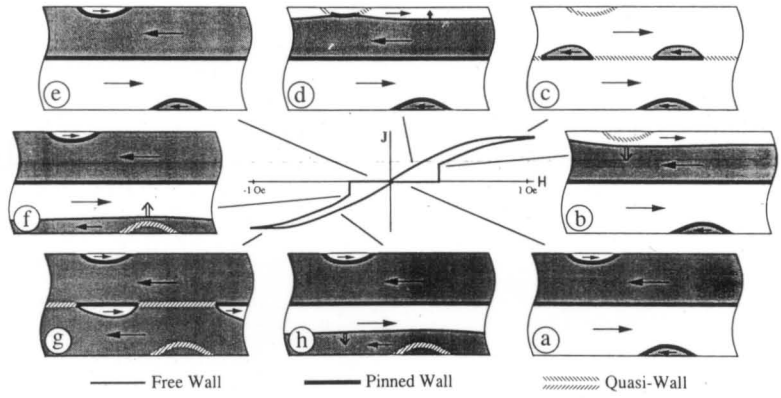

Fig. 15. Schematic summary of the domain configuration in a ribbon with a Perminvar loop for various applied fields as indicated: (a) demagnetized, (b) reentrant reversal to right, (c) soft saturation, (d) demagnetized return, (e) demagnetized, (f) reentrant reversal to left, (g) soft saturation, (h) demagnetized return.

the already mentioned curved profile of the sample edge. At a critical field—the coercivity of the pinned loop—the wall breaks suddenly free. As this is an instantaneous process that cannot be resolved in the digitally enhanced Kerr microscope, we cannot really decide at which point of the sample edge the wall breaks off first. It might be possible that free nucleation from the irregular sample edge plays a role too.

Careful observation of the domain behavior on a larger scale leaves no doubt that the remagnetization in the second half of the hysteresis begins at the sample edge rather than at the pinning site or at the ends of the sample. The details, including the origin of the observed jitter in the threshold field for the second half of magnetization reversal, are still uncertain.

3. Summary of the Pinned Loop Mechanism: With the knowledge about the nature of the residual and edge domains we can summarize the course of magnetization in the Perminvar mode. This is done schematically in Fig. 15. In the demagnetized state (Fig. 15(a)) all pinning sites are occupied by walls. When the field exceeds the threshold (Fig. 15(b)) the upper half of the sample is remagnetized in a reentrant way after some mode of nucleation from the sample edge, in which pinned edge domain might play a role. In the center of the sample, residual domains remain (Fig. 15(c)) stabilized mainly by ripple-like anisotropy modulations in the domains along the pinning site and secondarily by repulsive wall interactions. In the reverse half of the cycle these domains grow by movement of the free wall, leaving a stable pinned wall at the pinning site (Fig. 15(d)). The free wall moves to the sample edge to disappear there or to be pinned at the edge pinning sites (Fig. 15(e)). The process is now ready to repeat.

Of course the high nucleation field can only be realized if the sample ends do not act as nucleation centers. This is no problem since the structure of the transverse closure domains, which have to be present in the demagnetized state at the sample ends, are also annealed-in and stabilized during the heat treatment. Thus the ends are passivated and are not able to contribute to the remagnetization process in the center of the sample.

F. Mechanism of the Regular Loop

After a large longitudinal field completely saturated the sample and residual domains have been eliminated, the remaining quasi-wall at the pinning site becomes a nucleation source for remagnetization. Nucleation can occur preferentially at annealed-in cap switch points in the quasi-wall. Fig. 16(a) is a picture of the pinning site just as it appears as a quasi-wall after reducing the field from saturation. Two cap switches can be seen in the quasi-wall. As the field is further reduced, domains are nucleated with their free wall above the pinning site as in Fig. 16(b) or below the pinning site as in Fig. 16(c). The selection of the side seems to be random.

An example for the domain growth is shown in Fig. 17.

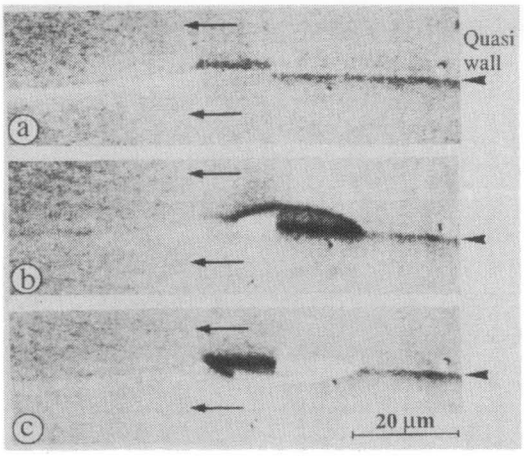

Fig. 16. Kerr magnetooptic micrograph of (a) a quasi-wall with cap switch, (b) nucleation site on one side, or (c) on the other side.

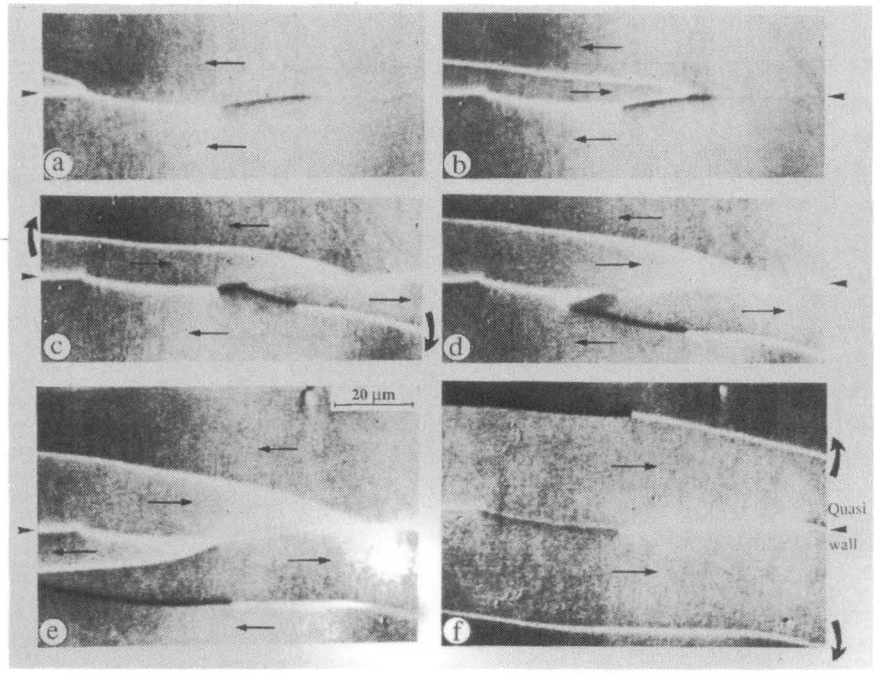

Fig. 17. Kerr magnetooptical micrographs of a section of a pinning site as domains grow on both sides: (a) quasi-wall, (b) domains grow leaving unstable cap, (c) to (d) domains grow on other side of pinning site until (f) complete quasi-wall is formed at the pinning site.

A section of quasi-wall with a reverse domain to the left is shown in Fig. 17(a). The domains grow along the quasi-wall, leaving behind pinned wall segments as seen in Fig. 17(b). Sometimes an unstable cap is formed on the pinned wall as can be seen. Reversal continues with a reverse domain growing on the other side of the pinning site as in Fig. 17(c). This process converts the unstable cap to a quasi-wall. The domains continue to grow as can be seen in the sequence Fig. 17(d), Fig. 17(e), and Fig. 17(f). Finally, a quasi-wall is left as seen in Fig. 17(f) that is surrounded by magnetization that is opposite to that in beginning, ready for a new reversal.

A summary of the mechanism of the regular loop is given in Fig. 18. Coming back from saturation, quasi-walls are formed at all pinning sites as shown in Fig. 18(a). Nucleation starts at annealed-in cap switch points on both sides of the quasi-walls (Fig. 18(b)). The domains grow (Fig. 18(c), 18(d)) and both halves of the sample are reversed simultaneously (Fig. 18(e)). After every magnetization cycle, a quasi-wall and some residual domains are left at the pinning site (Fig. 18(f), 18(b)). Remagnetization starts from these domains.

Conclusion

The mechanisms leading to a complicated hysteresis behavior of very low magnetostriction amorphous ribbons annealed in the demagnetized state have been clarified in detail for the first time. Digitally enhanced high resolu-

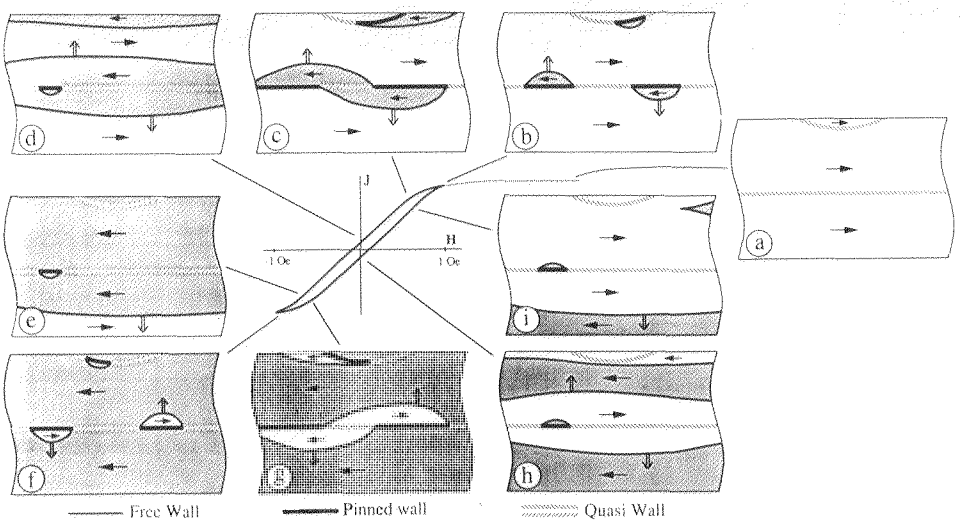

Fig. 18. Schematic summary of the domain configuration in a ribbon with a regular loop for various fields applied as indicated by the position on the loop.

tion Kerr microscopy was used. It was found that, for these thick ribbons, the Néel-like surface components of the wall exhibit all of the structure predicted by the stray field-free wall model and that all structure could be identified. By applying small fields a Perminvar-type hysteresis loop is maintained, stabilized by a pinned wall in the middle of the sample. The characteristic discontinuity in the magnetization curve is triggered by nucleation from the sample edges. Ripple-like anisotropy modulations in the domains along the pinning site and repulsive wall interactions are important for the stability of this state. If the ribbon is saturated longitudinally, all history is removed and the pinning site becomes a source of reverse domains for low coercive force reversal.

References

[1] H. Fujimori, H. Yoshimoto, and T. Masumoto, "Anomalous eddy current loss and amorphous magnetic materials with low core loss," *J. Appl. Phys.*, vol. 52, pp. 1893–1896, 1981.

[2] F. E. Luborsky and J. L. Walter, "Magnetic anneal anisotropy in amorphous alloys," *IEEE Trans. Magn.*, vol. MAG-13, pp. 953–956, 1977.

[3] J. Yamasaki, K. Mohri, K. Watari, and K. Narita, "Domain wall induced anisotropy during annealing in amorphous ribbons," *IEEE Trans. Magn.*, vol. MAG-20, pp. 1855–1857, 1984.

[4] W. K. Ho and F. B. Humphrey, "Domain wall pinning in sputtered soft amorphous magnetic thin films," *J. Appl. Phys.*, vol. 63, pp. 2944–2946, 1988.

[5] F. Schmidt, W. Rave, and A. Hubert, "Enhancement of magneto-optical domain observation by digital image processing," *IEEE Trans. Magn.*, vol. MAG-21, pp. 1596–1598, 1985.

[6] A. Hubert, *Theorie der Domänenwände in geordneten Medien*. Berlin-Heidelberg-New York: Springer-Verlag, 1974.

[7] D. A. Herman, Jr., B. E. Argyle, and B. Petek, "Bloch lines, cross ties and taffy in Permalloy," *J. Appl. Phys.*, vol. 61, pp. 4200–4206, 1987.

[8] P. J. Ryan and T. B. Mitchell, "Wide domain walls and Bloch lines in permalloy and Co–Fe films using Kerr effect microscopy," *J. Appl. Phys.*, vol. 63, pp. 3162–3164, 1988.

[9] J. Pfannenmüller, W. Rave, and A. Hubert, "Measuring the surface domain wall width by magneto-optics methods," presented at the 12th Int. Coll. Magn. Films Surfaces, Le Creusot, 1988, Conf. Abst., Paper TP-14.

[10] M. Paulus and W. Simonet, "Origine des parois kπ et des parois mobiles dans un ferrite a anisotropie induite," *J. de. Physique*, vol. 28, pp. 653–660, 1967.

[11] C. Aroca, P. Sanchez, and E. López, "Interaction of a Bloch domain wall with the helical anisotropy induced by itself," *Phys. Rev. B.*, vol. 34, pp. 490–493, 1986.

[12] S. Shtrikman and D. Treves, "Internal structure of Bloch walls," *J. Appl. Phys.*, vol. 31, pp. 147S–148S, 1960.

[13] U. Hartmann and H. H. Mende, "Hysteresis of Néel-line motion and effective width of 180° Bloch walls in bulk iron," *Phys. Rev. B.*, vol. 33, pp. 4777–4781, 1986.

[14] W. Rave, R. Schäfer, and A. Hubert, "Quantitative observation of magnetic domains with the magneto-optical Kerr effect," *J. Magn. Magn. Mat.*, vol. 65, 7–14, 1987.

Rudolf Schäfer was born in Sachsendorf, Germany, in 1960. He received the Ph.D. degree in engineering from the University of Erlangen in 1990.

Wing K. Ho was born in Hong Kong in 1963.

He received the M.S. degree in electrical engineering from Carnegie Mellon University, Pittsburgh, PA.

Since 1987, he has been affiliated with Sensormatic Electronics Corp. and has been working on the research and development of soft magnetic sensor material for the application of antishoplifting devices.

Mr. Ho is a member of the IEEE Magnetics Society and a member of Sigma Xi.

Jiro Yamasaki was born in Kumamoto, Japan, on February 27, 1946. He received the B.E., M.E., and Dr.E. degrees in electrical engineering from Kyushu University, Fukuoka, Japan, in 1971, 1974, and 1983, respectively.

From 1976 to 1983 he was a Research Associate at Kyushu University. In 1983 he joined the faculty at Kyushu Institute of Technology, Kitakyushu, Japan, where he is Professor of Department of Electrical Engineering. From 1986 to 1987 he was Visiting Scientist at the Magnetic Technology Center of Carnegie Mellon University, Pittsburgh, PA. Since 1974 he has worked on amorphous materials and its application.

Dr. Yamasaki is member of the IEEE Magnetics Society, IEE Japan, Magnetics Society of Japan and the Japan Society of Applied Physics.

Alex Hubert was born in Darmstadt, Germany, in 1938. He received the Ph.D. degree in physics from the University of Munich in 1965.

From 1966 to 1967 he was with the Max-Planck Institute for Metals Research in Stuttgart, Germany, and since 1976 he has been with the Institute of Materials Science of the University of Erlangen, where he is a Professor responsible for magnetic materials. His main interests are in the experimental and theoretical analysis of magnetic domains.

Floyd B. Humphrey was born in Greeley, CO, on May 20, 1925. He received the B.S. and Ph.D. degrees in physical chemistry from the California Institute of Technology, Pasadena, in 1950 and 1956, respectively.

In 1955 he joined the Solid-State Device Development Department of Bell Telephone Laboratories, Inc., Murray Hill, NJ, where he studied the relations between the structure and magnetic characteristics of ferrite and flux reversal in thin ferromagnetic films, and where he supervised the development of a permanent magnet twistor memory. In 1960 he joined the Jet Propulsion Laboratory and the California Institute of Technology. By 1964, he was full time on the campus, where he was a Professor of electrical engineering and applied physics. He continued his work on the dynamic characteristics of magnetic materials. He pioneered laser flash photography to actually see the dynamic domain configurations, studying first flux reversal in permalloy thin magnetic bubble wall dynamics. In 1980 he moved to Carnegie Mellon University, where he was Professor of electrical and computer engineering until September 1985, when he moved to the research track as a Senior Research Scientist. At CMU he continued the investigation of domain wall dynamics in magnetic bubble materials and bubble like devices, especially logic devices and VBL memory devices. In 1987 he joined the Boston University Electrical, Computer and Systems Department as a Research Scientist. He is studying domain wall structure using three-dimensional computer simulation.

Dr. Humphrey is a Fellow of the IEEE Magnetics Society and a member of Sigma Xi and the American Physical Society. He is the recipient of the IEEE 100th Anniversary Gold Medal and the IEEE Magnetics Society of 1988 Achievement Award.